

Research Article

Development of Aerosol Phospholipid Microparticles for the Treatment of Pulmonary Hypertension

Sarah Brousseau,¹ Zimeng Wang,¹ Sweta K. Gupta,¹ and Samantha A. Meenach^{1,2,3}

Received 17 April 2017; accepted 24 May 2017; published online 5 June, 2017

Abstract. Pulmonary arterial hypertension (PAH) is an incurable cardiovascular disease characterized by high blood pressure in the arteries leading from the heart to the lungs. Over two million people in the USA are diagnosed with PAH annually and the typical survival rate is only 3 years after diagnosis. Current treatments are insufficient because of limited bioavailability, toxicity, and costs associated with approved therapeutics. Aerosol delivery of drugs is an attractive approach to treat respiratory diseases because it increases localized drug concentration while reducing systemic side effects. In this study, we developed phospholipid-based aerosol microparticles via spray drying consisting of the drug tacrolimus and the excipients dipalmitoylphosphatidylcholine and dipalmitoylphosphatidylglycerol. The phospholipid-based spray-dried aerosol microparticles were shown to be smooth and spherical in size, ranging from 1 to 3 μm in diameter. The microparticles exhibited thermal stability and were amorphous after spray drying. Water content in the microparticles was under 10%, which will allow successful aerosol dispersion and long-term storage stability. In vitro aerosol dispersion showed that the microparticles could successfully deposit in the deep lung, as they exhibited favorable aerodynamic diameters and high fine particle fractions. In vitro dose-response analysis showed that TAC is nontoxic in the low concentrations that would be delivered to the lungs. Overall, this work shows that tacrolimus-loaded phospholipid-based microparticles can be successfully created with optimal physicochemical and toxicological characteristics.

KEY WORDS: pulmonary arterial hypertension; microparticles; aerosol delivery; spray drying; phospholipid.

INTRODUCTION

Pulmonary arterial hypertension (PAH) is a chronic, incurable cardiovascular disease with a 15% annual mortality rate. PAH involves an increase in pulmonary vascular resistance due to pulmonary arterial obstructions and can eventually lead to right ventricular failure and ultimately death. PAH is rare disease and approximately 2.4 new cases are diagnosed annually per million people (1) with a mean life expectancy of 3 years after diagnosis (2). It is likely that the worldwide impact of PAH is much more widespread than current diagnoses suggest due to the difficulty in accurately diagnosing patients. The characteristic pathogenesis of PAH is pulmonary arterial obstruction caused by vascular

proliferation and remodeling, which occurs in all layers of the vessel wall (3).

Current therapies for the treatment of PAH include prostanoids, endothelin receptor blockers, phosphodiesterase type 5 inhibitors, and soluble guanylate cyclase stimulators that are typically delivered orally or intravenously. These treatments are often expensive and difficult to deliver due to their limited bioavailability and toxicity of the drugs. Frequent dosing of these drugs is required because they have short half-lives. In addition, current therapies do not inhibit vascular remodeling and patients are often required to receive heart and lung transplantations to increase their chances of survival (4). The limited bioavailability of current PAH therapeutics and their associated toxicity results in the need for more sophisticated formulations to aid in patient compliance and health.

The lungs are an attractive approach for drug delivery because they are highly permeable and have a large surface area (35–140 m^2), allowing for higher bioavailability within the lungs (5). Targeted drug delivery to the lungs can be enhanced by using microparticle aerosols as they can effectively deposit in the lungs by impaction and physical

¹ Department of Chemical Engineering, University of Rhode Island, 51 Lower College Road, 215A Pastore Hall, Kingston, Rhode Island 02881, USA.

² Department of Biomedical and Pharmaceutical Sciences, University of Rhode Island, Kingston, Rhode Island 02881, USA.

³ To whom correspondence should be addressed. (e-mail: smeenach@uri.edu)

sedimentation (6). Nebulizers, pressurized metered dose inhalers, soft-mist inhalers, and dry powder inhalers (DPI) are among the most frequently used aerosol delivery devices. DPI are beneficial because they allow for the delivery of particles designed with specific characteristics (particle size, drug loading, etc.), and the resulting dry powder particles provide improved long-term chemical and physical stability (7). DPI are also advantageous because they are propellant-free, portable, easy to operate, and inexpensive (8).

The design specifications necessary for successful implementation in DPI can easily be met by using advanced spray drying techniques for the formation of dry powder aerosol particles. Spray drying can enable facile control of the size, surface morphology, and shape of spray-dried particles by altering component concentrations, drying temperature, pump rate, and gas flow of the spray dryer (9,10). Particle size and morphology play a large role in aerosol drug delivery (11). Optimally sized particles are within 1 to 5 μm for effective deep lung deposition (12). Particles below 5 μm can be easily deposited into the smaller airways, whereas submicron particles will be exhaled (11). Spray drying also increases the storage stability of particles due to the reduction in water content (13).

Bone morphogenic protein receptor type II (BMP2) is an active serine/threonine kinase receptor, which signals via the formation of heterocomplexes in response to ligands (3). BMP2 plays a large role in familial and idiopathic PAH (14). BMP2 gene mutations are found in more than 70% of cases of familial PAH and 10 to 40% of sporadic or anorexigen-associated PAH (15). In cases of PAH without a BMP2 mutation, BMP2 expression is still significantly reduced (3). Improving the signaling of BMP2 reduces damaging vascular remodeling and can potentially improve patient symptoms and outcomes (4).

Tacrolimus (TAC) (Fig. 1) is a poorly water-soluble immunosuppressive agent derived from the fungus *Streptomyces tsukubaensis* (16). It is normally delivered intravenously or orally but has poor bioavailability (17). TAC has a narrow therapeutic index, making it necessary to closely monitor patients for toxicity. Severe side effects have been shown to occur at blood concentrations greater than 50 ng/mL, which can easily occur during the initial phase of I.V. administration (18). By targeting the delivery of TAC to the lung, the systemic peak concentration of the drug could be greatly reduced, as seen with aerosolized fasudil (19). Nebulized TAC has been shown to improve the response of

a lung transplant patient while substantially reducing side effects (20). Blood levels have been found to remain low after the aerosolization of TAC, reaching 1.6 ng/mL after 12 h (21). While the systemic dose needed for PAH is currently unknown, the use of aerosolized microparticles capable of controlled delivery of TAC has the potential to decrease the peak systemic concentration of the therapeutic compound while providing an optimal systemic dose over a prolonged period of time. In addition, the use of a long-acting dry powder aerosol delivered via a DPI will provide a significant convenience and quality of life to PAH patients. TAC has been found to be effective in the treatment of pulmonary arterial hypertension by inducing the signaling of BMP2 in endothelial cells (4,14). While there have been several system delivery therapeutics for PAH (22–24), there exists a need for a lung-compatible, controllable aerosol drug delivery vehicle.

In this study, the TAC was spray-dried with the excipients dipalmitoylphosphatidylcholine (DPPC) and dipalmitoylphosphatidylglycerol (DPPG) to produce dry powder aerosol microparticles. DPPC and DPPG are phospholipid components naturally present in the lungs. Approximately 60% of PC in the lungs is composed of DPPC (25). Phospholipids such as DPPC and DPPG are necessary to support proper lung surfactant function (7) and help protect against infections and inflammation (26). Phospholipids are an efficient excipient because they protect the structural integrity, stability, and fluidity of the drug (27). Using phospholipid excipients that are biocompatible and biodegradable can aid in the delivery of drugs to the lungs by improving particle and drug migration to the lungs because of the reduction in surface tension from the surfactant (25,28,29). Phospholipid excipients may also cause the spray-dried particles delivered to the lungs to evade recognition and uptake by the immune system, increasing lung residence time (30). The chemical structures of DPPC and DPPG can be seen in Fig. 1.

The overall objective of this research was to develop and characterize phospholipid-based aerosol microparticles loaded with tacrolimus for applications in the treatment of PAH. The specific objectives of this research include (1) synthesis and optimization of phospholipid-based aerosol microparticles containing TAC using advanced spray drying methods, (2) evaluation of the physicochemical properties of the spray-dried microparticles, and (3) *in vitro* evaluation of the safety and efficacy of the fully characterized TAC-loaded aerosol microparticles.

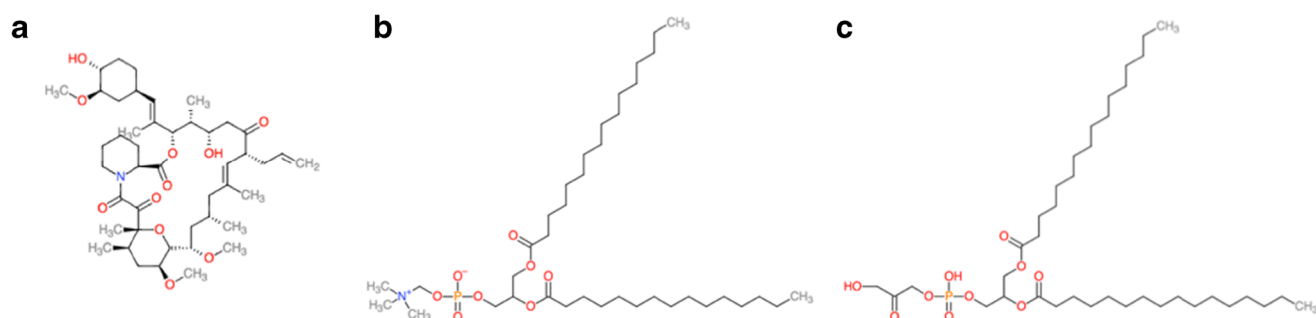


Fig. 1. Chemical structures of compounds used during manufacturing of spray-dried microparticles including: **a** tacrolimus (TAC), **b** dipalmitoylphosphatidylcholine (DPPC), and **c** dipalmitoylphosphatidylglycerol (DPPG)

MATERIALS AND METHODS

Materials

DPPC (>99%), DPPG (>99%), and 16:0–12:0 1-palmitoyl-2-[12-[(7-nitro-2-1,3-benzoxadiazol-4-yl)amino]dodecanoyl]-sn-glycero-3-phosphocholine (nitrobenzoxadiazole phosphatidylcholine (NBD-PC)) were obtained from Avanti Polar Lipids (Alabaster, AL, USA). TAC was obtained from LC Laboratories (Woburn, MA, USA). 2-Propanol (HPLC grade, 99.9%), Hydranal®-Coulomat, methanol (anhydrous, 99.8%), and acetonitrile (HPLC grade, ≥99.9%) were obtained from Sigma-Aldrich (St. Louis, MO, USA). Ultra-high purity (UHP) nitrogen gas was obtained from Airgas (Radnor Township, PA, USA). Extra pure phosphoric acid (85%) was obtained from Thermo Fisher Scientific (Waltham, MA). A549 cells were obtained from ATCC (Manassas, VA, USA). Sodium pyruvate was obtained from Fisher Scientific. Dulbecco's modified Eagle's medium (DMEM), Pen-Strep, and Fungizone® were obtained from Life Technologies (Norwalk, CT, USA). Sodium acetate (1 M, pH 5), Triton X-100, and dimethyl sulfoxide (DMSO) were obtained from Wilkem Scientific (Pawtucket, RI, USA). Fetal bovine serum (FBS) was obtained from Atlanta Biologics (Flowery Branch, GA, USA). Phosphate buffered saline (PBS), sodium hydroxide solution, and glycine were purchased from Fisher Scientific (Somerville, NJ).

Preparation of Spray-Dried Microparticles

Advanced spray drying of TAC and DPPC/DPPG particles was performed using a B-290 Mini Spray Dryer (Büchi Labortechnik AG, Switzerland) in closed mode. UHP dry nitrogen was used as the drying gas, and the spray-dried particles were collected in a sample collector. A nozzle with a diameter of 1.4 mm was used. The feed solutions were prepared by dissolving DPPC and DPPG in a 3:1 M ratio with varying amounts of TAC, including 0, 25, 50, 75, and 100 mol% TAC to the total amount of DPPC/DPPG in isopropanol to form a dilute solution of 0.5% w/v. The composition of each feed solution can be seen in Table I. The spray drying conditions used during particle formation were a pump rate of 100%, aspiration rate of 100%, and inlet temperature of 100°C. All spray-dried powders were stored

in small glass vials sealed with parafilm in desiccators at –20°C under ambient pressure.

Scanning Electron Microscopy

The shape and surface morphology of the spray-dried particles were evaluated via scanning electron microscopy (SEM) using a Zeiss SIGMA VP Field Emission Scanning Electron Microscope (Germany). Dry powder samples were placed on aluminum stubs (Ted Pella Inc., Redding, CA, USA) with double-sided adhesive carbon tabs and then coated with a thin film of a gold/palladium alloy using a BIO-RAD sputter coating system at 20 μÅ for 60 s under argon gas. Micrographs were collected at several different magnifications. The size of the spray-dried particles was analyzed using ImageJ Size Analysis software (31) with images obtained from the SEM at ×10 magnification. Fifty particles per sample were analyzed.

Differential Scanning Calorimetry

Thermal analysis and phase transition measurements of the raw materials and spray-dried particles were carried out via differential scanning calorimetry (DSC) using a DSC Q10 (TA Instruments, New Castle, DE, USA). One to two milligrams of the sample was weighed and sealed into aluminum Tzero pans with Tzero hermetic lids (TA Instruments). The samples were exposed to a heating range of –25 to 200°C at a heating scan rate of 5°C/min under UHP nitrogen gas.

Powder X-Ray Diffraction

Powder X-ray diffraction (PXRD) patterns of raw materials and particle powder samples were measured using a Rigaku Multiflex X-ray diffractometer (the Woodlands, TX, USA) with a slit-detection Cu Kα radiation source (40 kV, 44 mA, and λ = 1.5406 Å). The scan range was 5–30° in 2θ with a scanning rate of 2°/min at ambient temperature. The sample was placed on a horizontal quartz glass sample holder plate.

Table I. Systems of Spray-Dried Phospholipid-Based Particles and Their Corresponding Mol% of Tacrolimus, Dipalmitoylphosphatidylcholine, and Dipalmitoylphosphatidylglycerol, Outlet Temperature from the Spray Dryer, Geometric Diameter, Water Content, Drug Loading, and Encapsulation Efficiency

System	0TAC	25TAC	50TAC	75TAC	100TAC
TAC (mol%)	0	25	50	75	100
DPPC (mol%)	75	56.25	37.5	18.75	0
DPPG (mole %)	25	18.75	12.5	6.25	0
Outlet <i>T</i> (°C)	45	43	44	42	42
Diameter (μm)	N/A	1.5 ± 0.6	2.3 ± 0.6	2.3 ± 1.1	1.9 ± 0.8
Water content (%)	10.0 ± 3.3	6.8 ± 1.3	6.0 ± 2.5	6.7 ± 2.9	4.2 ± 1.5
TAC loading (mg TAC/mg particles)	N/A	0.29 ± 0.01	0.56 ± 0.04	0.54 ± 0.02	1.00 ± 0.01
TAC EE (%)	N/A	114.2 ± 8.8	111.3 ± 2.6	72.0 ± 8.7	100.2 ± 5.4

TAC tacrolimus, DPPG dipalmitoylphosphatidylglycerol, DPPC dipalmitoylphosphatidylcholine, EE encapsulation efficacy

Karl Fischer Coulometric Titrations

The water content of the raw materials and spray-dried particles was determined by Karl Fischer (KF) coulometric titration. The measurements were performed with an 851 Titrando KF Coulometer coupled with an 803 Ti Stand (Metrohm Ltd., Antwerp, Belgium). Approximately 10 mg of powder was dissolved in anhydrous methanol. The sample solution was then injected into the reaction cell containing Hydranal® and the water content was calculated from the resulting reading.

In Vitro Aerosol Dispersion Performance by the Next Generation Impactor™

The in vitro aerosol dispersion of the spray-dried microparticles was determined using a model 170 Next Generation Impactor™ from MSP Corporation (Shoreview, MN, USA) with a USP stainless steel induction port. The Next Generation Impactor™ (NGI™) was coupled with a Copley HCP5 vacuum pump and a Copley TPK 2000 critical flow controller (Copley Scientific, UK). The airflow rate was set to 60 L/min in order to model the airflow rate in the lung of a healthy adult (32). Glass fiber filters (55 mm, Type A/E, Pall Life Sciences, PA) were placed into the gravimetric insert cups and weighed before and after each experiment to determine particle deposition on each stage. Approximately 10 mg of microparticles was loaded into a hydroxypropyl methylcellulose capsule (HPMC, size 3, Quali-V®, Qualicaps® Inc., Whitsett, NC) and then placed into a dry powder inhaler (HandiHaler, Boehringer Ingelheim Pharmaceuticals, CT). The dry powder inhaler was attached to a rubber mouthpiece attached to the induction port on the NGI™. The NGI™ was operated with a 10 s delay and 10-s run time. The effective cutoff diameters for each stage of the NGI™ were given by the manufacturer as follows: stage 1 (8.06 μm), stage 2 (4.46 μm), stage 3 (2.82 μm), stage 4 (1.66 μm), stage 5 (0.94 μm), stage 6 (0.55 μm), and stage 7 (0.34 μm). The mass median aerodynamic diameter (MMAD) and geometric standard deviation (GSD) were calculated using a Mathematica® program written by Dr. Warren Finlay (33). The fine particle dose (FPD), fine particle fraction (FPF), respirable fraction (RF), and emitted dose (ED) were calculated using the following equations:

$$\text{FPD} = \text{Mass of particles on stages 2 through 7}$$

$$\text{FPF} = \frac{\text{FPD}}{\text{Initial particle mass loaded into capsules}} \times 100\%$$

$$\text{RF} = \frac{\text{FPD}}{\text{Total particle mass on all stages}} \times 100\%$$

$$\text{ED} = \frac{\text{Initial mass in capsules} - \text{Final mass remaining in capsules}}{\text{Initial mass in capsules}} \times 100\%$$

Drug Loading and Encapsulation Efficiency

Drug loading and encapsulation efficacy (EE) of TAC microparticles were determined via Ultra-Performance Liquid Chromatography (UPLC) (LaChrom, Hitachi, Japan).

Detection of TAC was performed using the following conditions: C₁₈, 5 μm × 150 mm × 4.6 mm column (Ascentis, Sigma-Aldrich, St. Louis, MO), 1 mL/min pump rate, 6 min retention time, mobile phase of 70% acetonitrile and 30% phosphoric acid aqueous solution (0.1%), absorbance of 215 nm, and temperature of 50°C. The experimental drug concentration in the microparticles was compared to a standard curve of drug in the mobile phase. Drug loading (DL) and EE were calculated using the following equations:

$$\text{DL} = \frac{\text{Actual drug mass}}{\text{Initial particle concentration}}$$

$$\text{EE} = \frac{\text{Actual drug mass}}{\text{Theoretical drug mass}} \times 100\%$$

In Vitro Cellular Viability

A549 lung adenocarcinoma cells were used to evaluate microparticle-cellular interactions. A549 cells were maintained in DMEM media supplemented with 10% (v/v) fetal bovine serum, 100 U/mL penicillin, 100 μg/mL streptomycin, fungizone® (0.5 μg amphotericin, B, 0.41 μg/mL sodium deoxycholate), and 1 mM sodium pyruvate.

The effect of raw TAC and TAC microparticles (MP) on A549 cell viability was determined. The cells were seeded at 5 × 10⁴ cells/mL (100 μL/well) in 96-well plate and incubated overnight at 37°C. Cells were then exposed to varying concentrations of raw TAC and the microparticle formulations (0.00001 to 10 μM). Twenty-four, 48, and 72 h after TAC exposure, the viability of the A549 cells was determined using a resazurin assay. Twenty microliters of resazurin solution (60 μM) was added to each well, and after 3 h, the fluorescence intensity of the resorufin produced by viable cells was detected at 520 nm (excitation) and 590 nm (emission) using a Cytation 3 plate reader (BioTek, Winooski, VT, USA). The relative viability of each sample was calculated using the following equation:

$$\text{Relative viability} = \frac{\text{Sample fluorescence intensity}}{\text{Control fluorescence intensity}} \times 100$$

In Vitro Cellular Uptake of TAC Microparticles

To study the cellular uptake behavior, A549 cells were exposed to different TAC MP formulations. Cells were seeded at 5 × 10⁴ cells/mL (100 μL/well) in 96-well plate and incubated overnight at 37°C. Twenty-four hours after exposure, the medium was discarded and A549 cells were washed three times with 1× PBS to remove excess microparticles in the wells. To calculate the uptake of the microparticles in the cells, the cells were lysed using 50 μL of 0.5% Triton X-100 in 0.2 N NaOH for 30 min. Subsequently, 200 μL of UPLC mobile phase (acetonitrile and 0.3% phosphoric acid) was added to the tube of cells and was centrifuged at 10,000 rpm for 15 min. The supernatant was collected to analyze the concentration of TAC via UPLC.

In addition, A549 cells were seeded at 1×10^6 cells/mL (100 μ L/well) in a six-well plate and incubated overnight at 37°C. The cells were then exposed to 10 μ M of fluorescently labeled TAC MP in media for 3, 6, and 24 h. The microparticles were formulated as previously described with the addition of 1 mol% of NBD-PC fluorophore to allow for fluorescent imaging of the particles. After exposure, the particle solution was removed and the cells were washed twice with 200 mM glycine to remove any unbound particles. They were then washed with $1 \times$ PBS and fixed with 75% ethanol for 15 min. The images were captured using a Biotek Cytation 3 imaging system.

RESULTS AND DISCUSSION

The described study involved the physicochemical and in vitro characterization of TAC-loaded phospholipid particles produced via spray drying. Optimization and design resulted in the formulation of several MP systems, which included four systems loaded with TAC (25, 50, 75, and 100 mol% TAC) and one without TAC (consisting of pure phospholipids). This study strived to determine the effects on the presence of differing TAC amounts on the particle formulations. The size, morphology, thermal stability and

crystallinity, water content, aerodynamic dispersion performance, and in vitro effects on pulmonary cells were evaluated.

Size and Morphology

The size and morphology of the formulated particles were analyzed using SEM micrographs, as seen in Fig. 2. The geometric diameter of the particles is displayed in Table I and was determined using ImageJ software. 0TAC particles were agglomerated and as a result their diameter was immeasurable. 25TAC and 75TAC particles were rounder and smoother than 0TAC with some agglomeration and sintering between particles. 50TAC particles were spherical, smooth, and relatively uniformly sized. 100TAC particles were round and smooth but not uniformly sized. The geometric diameter of all measurable particles was between 1.5 and 2.3 μ m, where 50TAC particles were the largest and 100TAC particles were the smallest.

Thermal Analysis

DSC studies were performed on the raw materials prior to spray drying (TAC, DPPC, DPPG) and spray-dried

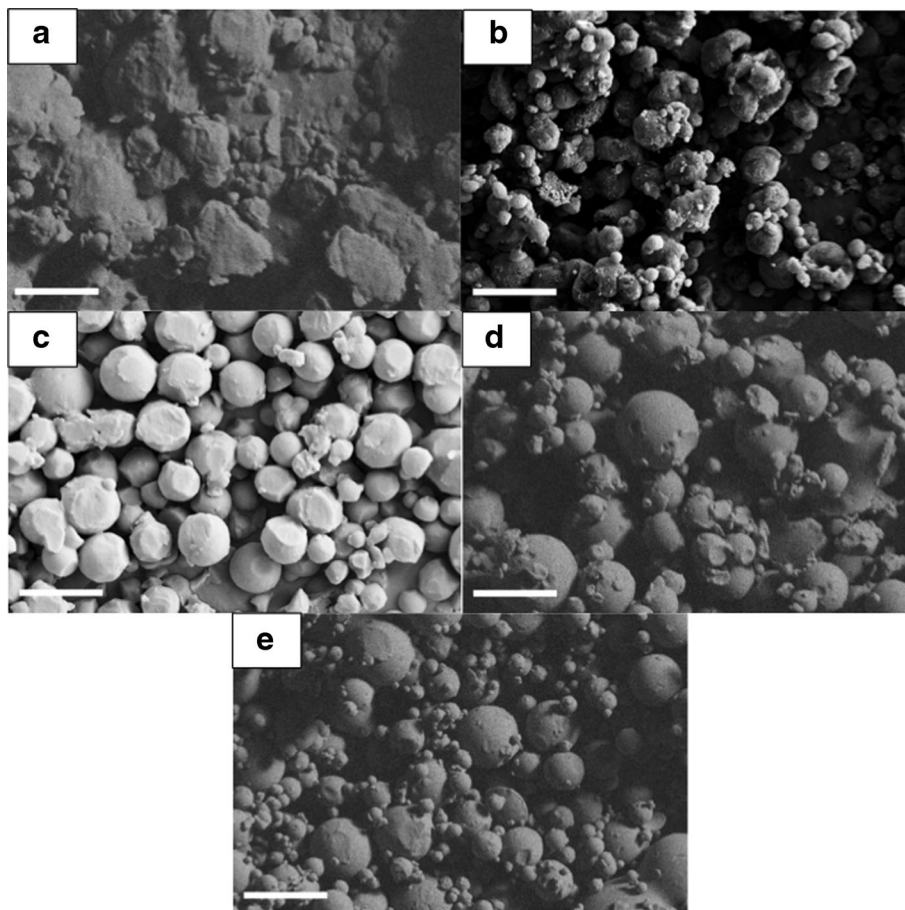


Fig. 2. Representative scanning electron microscopy (SEM) micrographs of spray-dried phospholipid-based microparticles: **a** 0TAC, **b** 25TAC, **c** 50TAC, **d** 75TAC, and **e** 100TAC, where the *number* indicates the mole percentage of TAC in each system. Magnification = $\times 10,000$. Scale bar = 5 μ m

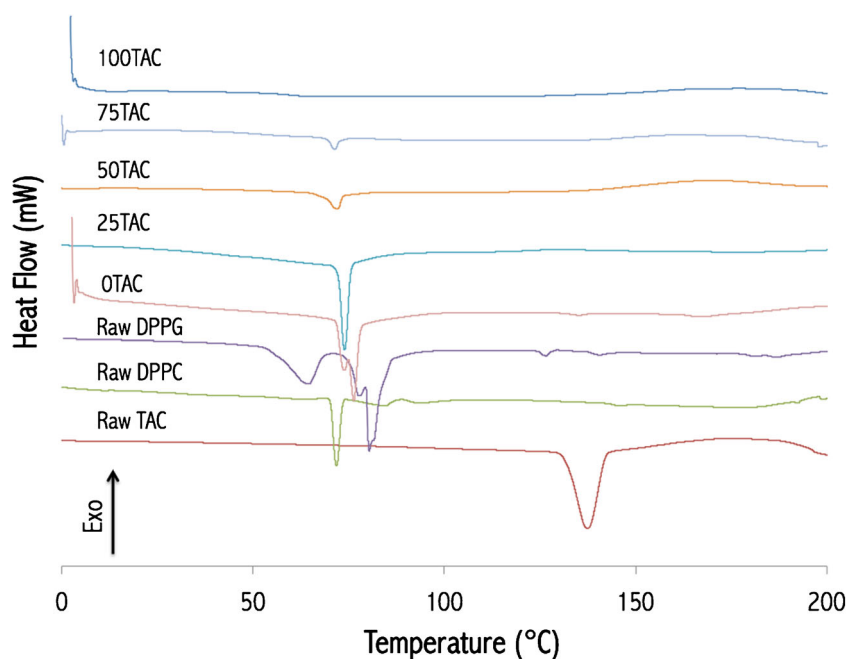


Fig. 3. Differential scanning calorimetry (DSC) thermograms of spray-dried microparticles of varying compositions and their corresponding raw materials

microparticles (0TAC, 25TAC, 50TAC, 75TAC, and 100TAC) to determine their thermal behavior and melting points, as seen in Fig. 3. An endothermic peak is evident at 129°C for raw TAC, signifying its melting point. The endothermic peak signifying the TAC melting point is not present in the thermograms of the spray-dried particles due to the transition of TAC from crystalline to amorphous forms during the spray drying process. Raw DPPC and DPPG exhibited characteristic bilayer main phase transitions at 71 and 79°C, respectively (34). A bilayer main phase transition was also seen in the spray-dried microparticles at

approximately 76°C, becoming less prevalent with increasing drug concentration due to the DPPC content.

The formulated microparticles were spray-dried at an inlet temperature of 100°C at a pump rate of 100% (the highest possible for the described system). As a result, the outlet temperatures of the spray drying process for the microparticles ranged from 42 to 45°C, as seen in Table I. These outlet temperatures are below the phase transition temperatures as indicated in the DSC thermograms; therefore, the spray drying temperatures do not negatively impact the formation of the microparticles.

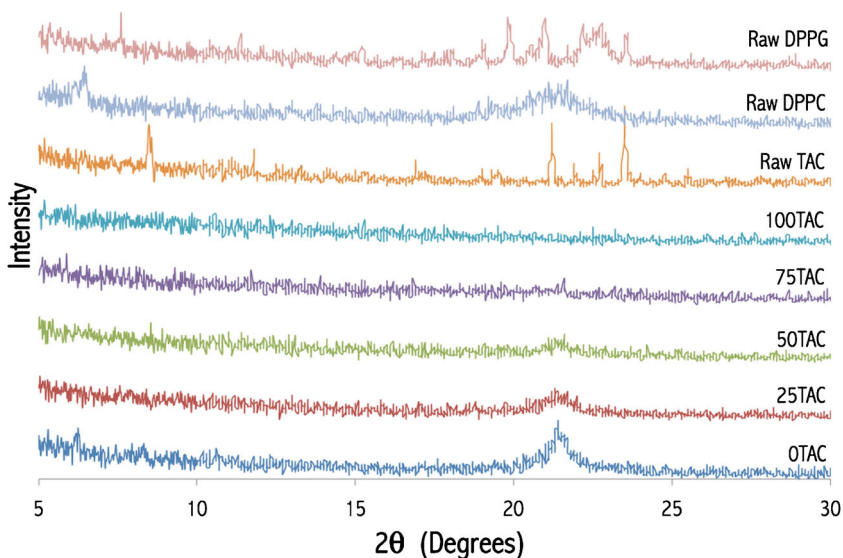


Fig. 4. X-ray powder diffractograms (XRD) of spray-dried microparticles with varying compositions and their corresponding raw materials

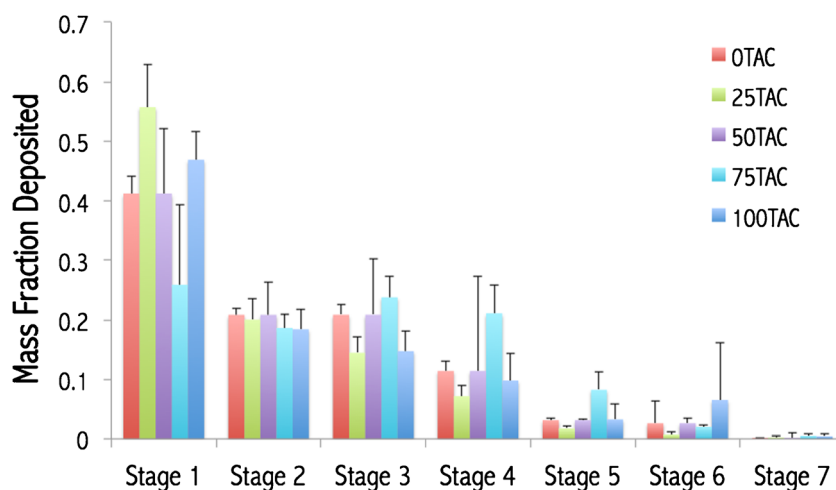


Fig. 5. *In vitro* aerosol dispersion performance as mass fraction of microparticles deposited on each stage of the Next Generation Impactor™ (NGI™) for spray-dried particles containing DPPC and DPPG with varying TAC content. For $Q = 60$ L/min, the effective cutoff diameters (D_{50}) for each NGI™ impaction stage are as follows: stage 1 (8.06 μm), stage 2 (4.46 μm), stage 3 (2.82 μm), stage 4 (1.66 μm), stage 5 (0.94 μm), stage 6 (0.55 μm), and stage 7 (0.34 μm). ($n = 3$, average \pm SD)

Crystallinity Analysis

X-ray powder diffractograms were collected for the raw components (TAC, DPPC, DPPG) and spray-dried microparticles (0TAC, 25TAC, 50TAC, 75TAC, and 100TAC) as shown in Fig. 4. Strong peaks are seen in raw TAC between 20 and $25^\circ 2\theta$, indicating the crystallinity of the material prior to the spray drying process. Raw DPPC exhibited a strong broad peak at $21^\circ 2\theta$, which corresponds to the presence of the phospholipid bilayer structure (27). Raw DPPG showed a cluster of peaks between 18° and $25^\circ 2\theta$. The spray-dried particles show decreasing peak intensities at $22^\circ 2\theta$ with increasing mole percentage of TAC. The peaks corresponding to raw DPPG were not noticeable in the spray-dried formulations, likely due to their limited presence in comparison to raw DPPC, which has a strong peak signal. 0TAC and 25TAC exhibited the most evident peaks of the spray-dried particles at $22^\circ 2\theta$, indicative of the presence of phospholipid bilayer structures within the particles. The lack of

significant peaks in the 50TAC, 75TAC, and 100TAC particles is likely due to the lower mole percentage of the phospholipids and reveals that the TAC present in the spray-dried particles is amorphous. Amorphous solids are more soluble and have higher dissolution rates than crystalline solids, which is favorable for aerosol formulations (27).

Overall, PXRD and DSC analysis indicates that the spray-dried phospholipid TAC-loaded microparticles display the characteristics of particles with a lipid bilayer structure (likely multilamellar) owing to the signature peaks in XRD analysis and bilayer phase transition values in the DSC thermograms (26,35).

Water Content

The residual water content in the spray-dried microparticles can be seen in Table I. The water content in the microparticles ranged from 4 to 10%. It was the highest in 0TAC particles, at 10.0%, and lowest in the 100TAC

Table II. *In Vitro* Aerosol Dispersion Performance Using the Next Generation Impactor™ for Spray-Dried Phospholipid-Based Systems Containing Tacrolimus

System	0TAC	25TAC	50TAC	75TAC	100TAC
MMAD (μm)	4.0 \pm 0.6	9.1 \pm 2.2	8.7 \pm 5.2	4.1 \pm 0.7	6.0 \pm 1.8
GSD (μm)	2.1 \pm 0.2	2.5 \pm 0.4	2.5 \pm 0.5	2.1 \pm 0.2	2.9 \pm 0.9
Fine particle dose (mg)	8.7 \pm 1.3	6.4 \pm 1.1	5.2 \pm 2.5	9.5 \pm 0.8	8.8 \pm 1.3
Fine particle fraction (%)	29.4 \pm 4.7	20.9 \pm 3.3	10.0 \pm 0.2	32.1 \pm 1.68	29.0 \pm 4.7
Respirable fraction (%)	49.2 \pm 8.4	51.1 \pm 1.2	41.7 \pm 16.1	50.4 \pm 9.2	55.7 \pm 6.8
Emitted dose (%)	100 \pm 0.3	92.5 \pm 4.9	99.8 \pm 4.6	88.0 \pm 7.3	97.6 \pm 1.0

Parameters include mass median aerodynamic diameter, geometric standard deviation, fine particle fraction, respirable fraction, and emitted dose ($n = 3$, average \pm SD)

MMAD mass median aerodynamic diameter, GSD geometric standard deviation, FPF fine particle fraction, RF respirable fraction, ED emitted dose

particles, at 4.2%. The remaining formulations had 6–7% residual water, which is similar to previously reported results (7). Low water content in inhalable dry powders is essential for aerosol dispersion properties because it reduces agglomeration (30). High water content in aerosol powders and drug formulations can also reduce stability due to the propensity of amorphous powders to recrystallize in aqueous conditions (36).

In Vitro Aerosol Dispersion Analysis

The most important factor influencing the deposition of particulates in the lungs is the aerodynamic properties of the therapeutic system (32). The in vitro aerosol dispersion performance properties of the microparticles were

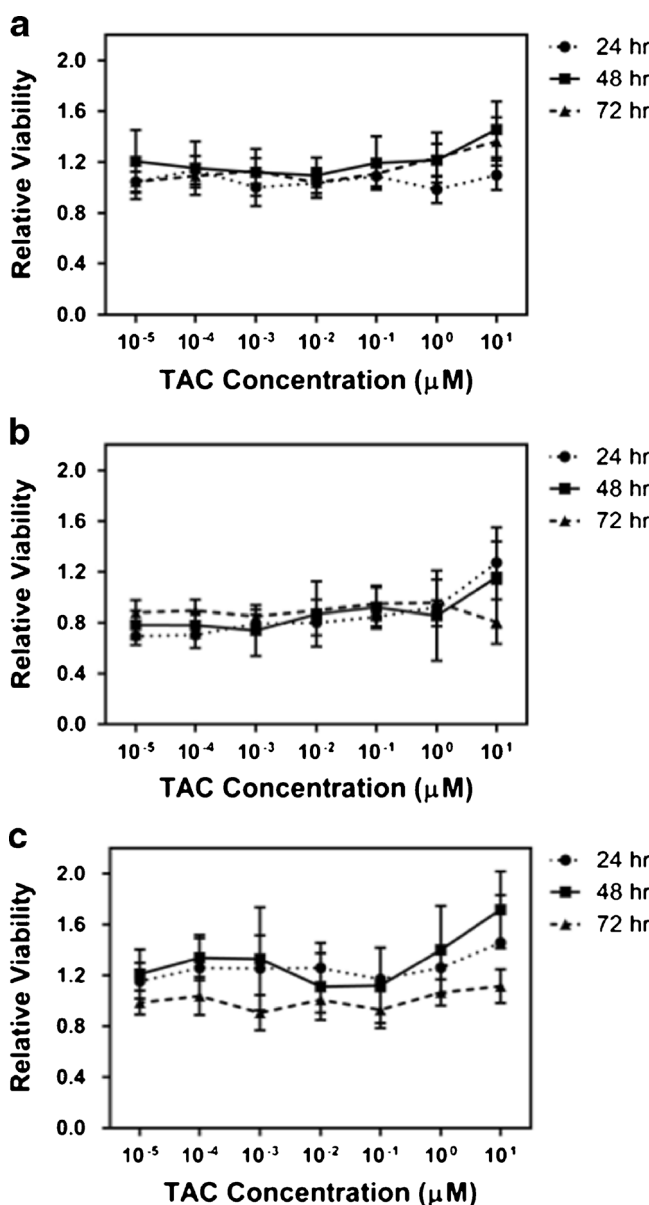


Fig. 6. Dose-response viability analysis of **a** raw TAC, **b** 50TAC, and **c** 75TAC microparticles on A549 lung adenocarcinoma cells at 24, 48, and 72 h

evaluated using an NGI™ coupled with a DPI device and can be seen in Fig. 5 and Table II. Figure 5 demonstrates the aerosol dispersion performance of the formulated dry powder microparticles by showing the mass fraction of particles on each NGI™ stage. The MMAD of the particles were 4.0 μm for 0TAC, 9.1 μm for 25TAC, 8.7 μm for 50TAC, 4.1 μm for 75TAC, and 6.0 μm for 100TAC. The GSD for the spray-dried microparticles ranged from 2.1 to 2.9 μm , and these values were similar to previously reported results (7). All particles were within the range for optimal deep lung deposition in children and

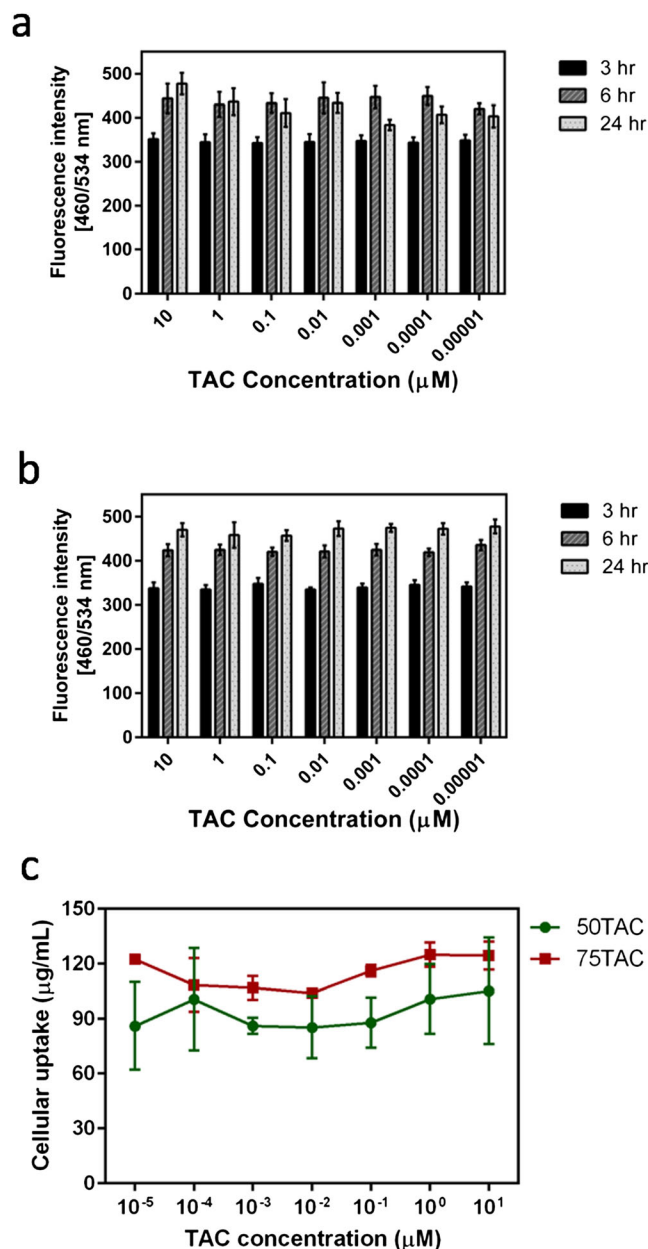


Fig. 7. Quantitative analysis of cellular uptake of TAC-loaded DPPC/DPPG microparticles (MP) by A549 cells by evaluating the fluorescence intensity of the MP via fluorescence microscopy for **a** 50TAC and **b** 75TAC at 3, 6, and 24 h and **c** via HPLC after 24 h of exposure. ($n = 3$, average \pm SD)

adults (12). The particles exhibited an ideal size range for ensuring targeted delivery to specific regions of the lung. In particular, the geometric diameters indicate that the described microparticles are capable of delivering a therapeutic payload to the deep lung (37), which is necessary for the treatment of PAH.

The FPF of the particles ranged from 10.0 to 32.1%, the respirable fractions (RF) ranged from 35.8 to 55.7%, and the ED ranged from 88 to 100%. In addition, as indicated in Fig. 5, 21–27% of microparticles deposited on stages 2 to 4 and 1–6% of MP deposited on stages 5 to 7. There were no clear trends corresponding to the effect of the amount of drug in relation to excipient on the aerosol dispersion properties of the microparticles. The particles with the most optimal aerosol performance were the 75TAC particles. Overall, aerosol dispersion was measurable on all of the NGI™ stages, and as a result, these microparticles are predicted to deposit in the deep lung region of the human lung as well as throughout the upper portions of the lung as indicated by the MMAD values.

Drug Loading and Encapsulation Efficiency

UPLC was used to evaluate the drug loading and encapsulation efficiency of tacrolimus in the spray-dried microparticles, which can be seen in Table II. Both drug loading and encapsulation efficiency were favorable for all particles containing TAC. The encapsulation efficiencies of 25TAC and 50TAC were above 100%, which is likely due to excipient loss during the spray drying process. Overall, the high EE values can allow for a smaller overall dosage of TAC MP to the lungs. The actual drug loading of 25TAC, 50TAC, and 100TAC was similar to their theoretical (initial) drug loading as shown by the EE values. 75TAC had a drug loading similar to 50TAC (0.54 and 0.56 mg TAC/mg particles, respectively). The difference in the ratio of excipient between these systems could explain the difference in some of the other results, including the aerosol dispersion performance of the particles.

In Vitro Cellular Viability

A dose-response study was completed by exposing A549 cells to different concentrations of raw TAC and TAC-loaded microparticles (50TAC and 75TAC) (Fig. 6). For raw TAC, the relative viability of the A549 cells remained constant for increasing drug concentrations at all exposure times, demonstrating that TAC is nontoxic to lung cells up to 10 μ M. 50TAC microparticles did not cause significant cytotoxic effects at various TAC concentrations until 72 h where there was a slight decrease in the viability of A549 cells. For 75TAC, the cell viability was not significantly affected at 24 and 48 h. At 72 h, there was a small decrease in viability. At higher concentrations (20 μ M), TAC becomes toxic to A549 cells (data not shown). However, since the amount of TAC delivered to the lungs can be well controlled, it can be ensured that concentration of TAC in the lungs would not exceed this range, particularly with spray-dried microparticles. Thus, delivering TAC to the lung as spray-dried microparticles is not expected to cause cell death, minimizing potential negative side effects.

In Vitro Cellular Uptake

The effect of the TAC-loaded microparticles on cellular uptake by A549 cells over time is shown in Fig. 7. In this study, A549 cells were exposed to 50TAC and 75TAC. For both microparticle formulations, there was no significant difference in the uptake with increasing concentrations, indicating that the uptake is not concentration dependent (Fig. 7). However, A549 cells showed higher cellular uptake for 75TAC as compared to 50TAC. The cells were also exposed to fluorescently labeled 50TAC and 75TAC. The resulting images demonstrated that after 3 h of incubation, the fluorescent 50TAC and 75TAC (green) were present in the cell cytoplasm. After 6 h, the particles started migrating towards the nucleus (Fig. 8). After 24 h of incubation, there was a strong fluorescence in the nucleus, indicating that the microparticles reached the nucleus. Figure 8 showed that 75TAC had higher fluorescence, demonstrating

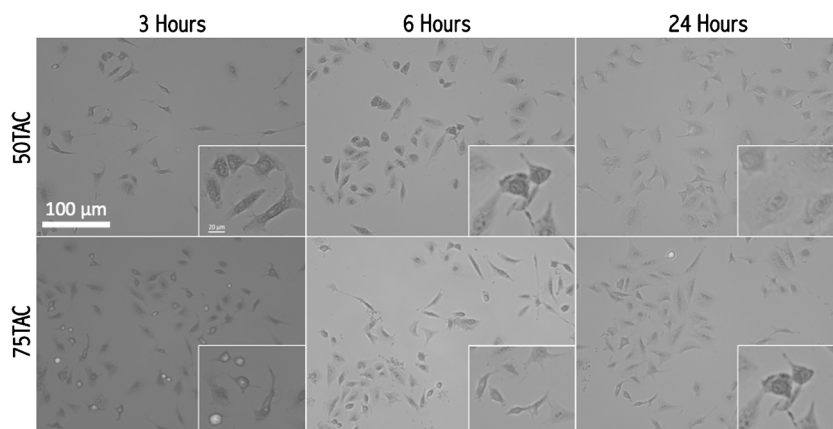


Fig. 8. Representative fluorescent and brightfield (overlay) images of A549 lung adenocarcinoma cells exposed to TAC/DPPC-DPPG microparticles loaded with a fluorescent dye after 3-, 6-, and 24-h exposure for 50TAC and 75TAC systems. The *inset* represents a zoomed in image of the cells and the inset *scale bar* = 20 μ m. ($n = 3$, average \pm SD)

higher cellular uptake compared to 50TAC after 24 h of exposure. This supports the aforementioned quantitative results. It can be concluded that TAC-loaded microparticles are able to reach the nucleus and have been taken up by the A549 cells.

CONCLUSIONS

Dry powder aerosol microparticles containing TAC, DPPC, and DPPG were successfully formulated via spray drying and exhibited optimal characteristics for use in the treatment of PAH. Five different MP formulations were produced with a 3 to 1 M ratio of DPPC to DPPG and varying TAC concentrations. The physicochemical characteristics of the microparticles were evaluated prior to *in vitro* cellular analysis. 0TAC did not form distinguishable microparticles, but the remaining MP formulations ranged from 1.5 to 2.5 μm in size. 50TAC and 75TAC particles were spherical and smooth with a narrow size distribution. The microparticles were found to be stable in the working temperature range with no measurable thermal degradation. The spray drying process resulted in amorphous microparticles, which can improve drug solubility. Water content in the microparticles was low, which is essential for dry powder aerosolization and formulation stability. The *in vitro* aerosol dispersion showed that these microparticles are optimal for deep lung deposition for drug delivery. Dose-response analysis showed that the concentrations of tacrolimus that will be present in the lungs would be nontoxic.

ACKNOWLEDGEMENTS

The authors gratefully acknowledge financial support from an Institutional Development Award (IDeA) from the National Institute of General Medical Sciences of the National Institutes of Health under grant number P20GM103430. The content is solely the responsibility of the authors and does not necessarily represent the official views of the National Institutes of Health. Finally, the authors thank RI-INBRE for UPLC access and RIN2 for SEM, PXRD, and DSC access.

COMPLIANCE WITH ETHICAL STANDARDS

Conflict of Interest No conflicts of interest exist.

REFERENCES

1. Archer S, Weir E, Wilkins M. Basic science of pulmonary arterial hypertension for clinicians new concepts and experimental theories. *Circulation*. 2010;121(18):2045–U175.
2. Saigal A, Ng WK, Tan RBH, Chan SY. Development of controlled release inhalable polymeric microspheres for treatment of pulmonary hypertension. *Int J Pharm*. 2013;450:114–22.
3. Humbert M, Morrell NW, Archer SL, Stenmark KR, MacLean MR, Lang IM, et al. Cellular and molecular pathobiology of pulmonary arterial hypertension. *J Am Coll Cardiol*. 2004;43(12s1):S13–24.
4. Spiekerkoetter E, Tian X, Cai J, Hopper R, Sudheendra D, Li C, et al. FK506 activates BMPR2, rescues endothelial dysfunction, and reverses pulmonary hypertension. *J Clin Investig*. 2013;123(8):3600–13.
5. Shoyele SA, Cawthorne S. Particle engineering techniques for inhaled biopharmaceuticals. *Adv Drug Deliv rev*. 2006;58:1009–29.
6. Li X, Mansour HM. Physicochemical characterization and water vapor sorption of organic solution advances spray-dried inhalable trehalose microparticles and nanoparticles for targeted dry powder pulmonary inhalation delivery. *AAPS PharmSciTech*. 2011;12(4).
7. Meenach SA, Vogt FG, Anderson KW, Hilt JZ, McGarry RC, Mansour HM. Design, physicochemical characterization, and optimization of organic solution advanced spray-dried inhalable dipalmitoylphosphatidylcholine (DPPC) and dipalmitoylphosphatidylethanolamine poly(ethylene glycol) (DPPE-PEG) microparticles and nanoparticles for targeted respiratory nanomedicine delivery as dry powder inhalation aerosols. *Int J Nanomedicine*. 2013;8:275–93.
8. Bosquillon C, Lombry C, Preat V, Vanbever R. Influence of formulation excipients and physical characteristics of inhalation dry powders on their aerosolization performance. *J Control Release*. 2001;70(3):329–39.
9. Iskandar F, Gradon L, Okuyama K. Control of the morphology of nanostructured particles prepared by the spray drying of a nanoparticle sol. *J Colloid Interface Sci*. 2003;265(3):296–303.
10. Hoe S, Ivey JW, Boraey MA, Shamsaddini-Shahrbabak A, Javaheri E, Matinkhoo S, et al. Use of a fundamental approach to spray-drying formulation design to facilitate the development of multi-component dry powder aerosols for respiratory drug delivery. *Pharm res*. 2014;31:449–65.
11. Chow AHL, Tong HHY, Chattopadhyay P, Shekunov BY. Particle engineering for pulmonary delivery. *Pharmaceutical Research*. 2007;24(3).
12. Meenach SA. High-performing dry powder inhalers of paclitaxel DPPC/DPPG lung surfactant-mimic multifunctional particles in lung cancer: physicochemical characterization, *in vitro* aerosol dispersion, and cellular studies. *AAPS PharmSciTech*. 2014;15(6):1574–87.
13. Ré M-I. Formulating drug delivery systems by spray drying. *Dry Technol*. 2006;24:433–46.
14. Hong K-H, Lee YJ, Lee E, Park SO, Han C, Beppu H, et al. Genetic ablation of the *Bmpr2* gene in pulmonary endothelium is sufficient to predispose to pulmonary hypertension. *Circulation*. 2008;118(7):722–30.
15. Humbert M, Sitbon O, Chaouat A, Bertocchi M, Habib G, Gressin V, et al. Survival in patients with idiopathic, familial, and anorexigen-associated pulmonary arterial hypertension in the modern management era. *Circulation*. 2010;122:156–63.
16. Cho JH. Development of novel fast-dissolving tacrolimus solid-dispersion-loaded prolonged release tablet. *Eur J Pharm Sci*. 2014:1–7.
17. Gao S, Sun J, Fu D, Zhao H, Lan M, Gao F. Preparation, characterization and pharmacokinetic studies of tacrolimus-dimethyl- β -cyclodextrin inclusion complex-loaded albumin. *Int J Pharm*. 2012;427:410–6.
18. Watts AB, Peters JI, Talbert RL, O'Donnell KP, Coalson JJ, Williams RO. Preclinical evaluation of tacrolimus colloidal dispersion for inhalation. *Eur J Pharm Biopharm*. 2011;77(2):207–15.
19. Gupta V, Gupta N, Shaik IH, Mehvar R, McMurtry IF, Oka M, et al. Liposomal fasudil, a rho-kinase inhibitor, for prolonged pulmonary preferential vasodilation in pulmonary arterial hypertension. *J Control Release*. 2013;167(2):189–99.
20. Hayes DJ, Zwischenberger JB, Mansour HM. Aerosolized tacrolimus: a case report in a lung transplant recipient. *Transplant Proc*. 2010;42:3876–9.
21. Schrepfer S, Deuse T, Reichenspurner H, Hoffmann J, Haddad M, Fink J, et al. Effect of inhaled tacrolimus on cellular and humoral rejection to prevent posttransplant obliterative airway disease. *Am J Transplant*. 2007;7(7):1733–42.
22. Wang Z, Cuddigan JL, Gupta SK, Meenach SA. Nanocomposite microparticles (nCmP) for the delivery of tacrolimus in the treatment of pulmonary arterial hypertension. *Int J Pharm*. 2016;512(1):305–13.

23. Chen L, Nakano K, Kimura S, Matoba T, Iwata E, Miyagawa M, et al. Nanoparticle-mediated delivery of pitavastatin into lungs ameliorates the development and induces regression to monocrotaline-induced pulmonary artery hypertension. *Hypertension*. 2011;57(2):343–50.
24. Kimura S, Egashira K, Chen L, Nakano K, Iwata E, Miyagawa M, et al. Nanoparticle-mediated delivery of nuclear factor κ B into lung ameliorates monocrotaline-induced pulmonary arterial hypertension. *Hypertension*. 2009;53(5):577–83.
25. Evora C, Soriano I, Rogers RA, Shakesheff KM, Hanes J, Langer R. Relating the phagocytosis of microparticles by alveolar macrophages to surface chemistry: the effect of 1,2-dipalmitoylphosphatidylcholine. *J Control Release*. 1998;51(2–3):143–52.
26. Mansour H, Wang DS, Chen CS, Zografi G. Comparison of bilayer and monolayer properties of phospholipid systems containing dipalmitoylphosphatidylglycerol and dipalmitoylphosphatidylinositol. *Langmuir*. 2001;17(21):6622–32.
27. Alves GP, Santana MHA. Phospholipid dry powders produced by spray drying processing: structural, thermodynamic and physical properties. *Powder Technol*. 2004;145:139–48.
28. Mansour HM, Sohn M, Al-Ghananeem A, DeLuca PP. Materials for pharmaceutical dosage forms: molecular pharmaceuticals and controlled release drug delivery aspects. *Int J Mol Sci*. 2010;11(9):3298–322.
29. Mansour HM, Xu Z, Meenach SA, Deluca PP. Novel drug delivery systems: inhalation aerosols, pulmonary/nasal drug delivery, and nanomedicine. In: Mitra A, editor. *Drug Delivery* 2013.
30. Meenach SA, Anderson KW, Hilt JZ, McGarry RC, Mansour HM. Characterization and aerosol dispersion performance of advanced spray-dried chemotherapeutic PEGylated phospholipid particles for dry powder inhalation delivery in lung cancer. *Eur J Pharm Sci*. 2013;49(4):699–711.
31. Abramoff MD, Magalhaes PJ, Ram SJ. Image processing with ImageJ. *Biophoton Int*. 2004;11(7):36–42.
32. Hickey AJ, Mansour HM. Delivery of drugs by the pulmonary route. In: Florence AT, Siepmann J, editors. *Modern pharmaceuticals*. 2. 5th ed. New York: Taylor and Francis; 2009. p. 191–219.
33. Finlay WH. *The mechanics of inhaled pharmaceutical aerosols: an introduction*. London: Academic Press; 2001.
34. Mansour HM, Zografi G. The relationship between water vapor absorption and desorption by phospholipids and bilayer phase transitions. *J Pharm Sci*. 2007;96(2):377–96.
35. Mansour HM, Zografi G. Relationships between equilibrium spreading pressure and phase equilibria of phospholipid bilayers and monolayers at the air-water interface. *Langmuir*. 2007;23:3809–19.
36. Wu X, Hayes DJ, Zwischenberger JB, Kuhn RJ, Mansour HM. Design and physicochemical characterization of advanced spray-dried tacrolimus multifunctional particles for inhalation. *Drug des Devel Ther*. 2013;7:59–72.
37. Sung JC, Pulliam BL, Edwards DA. Nanoparticles for drug delivery to the lungs. *Trends Biotechnol*. 2007;25(12):563–70.